

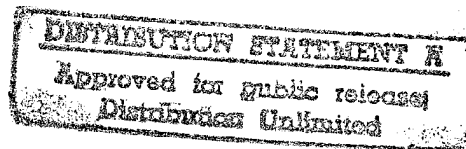
ADD 443233

NASA Technical Memorandum 4185

Fracture Toughness and  
Crack Growth of Zerodur

Michael J. Viens

APRIL 1990



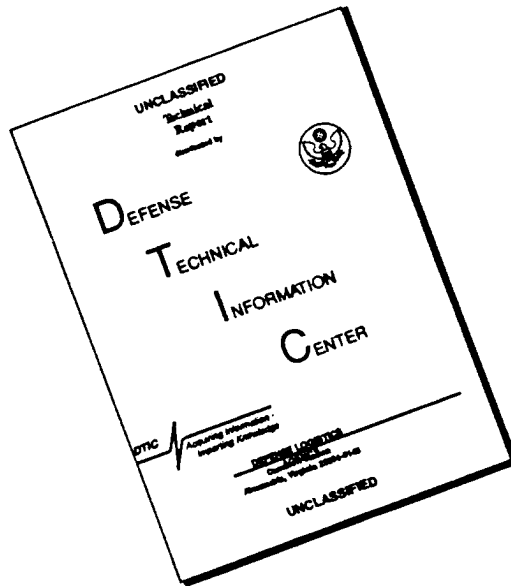
DEPARTMENT OF DEFENCE  
PLASTICS TECHNICAL EVALUATION CENTER  
ARDEC PICATINNY ARSENAL, N.J. 07806

**NASA**

19960612 035

CLASSIFIED 054126

# DISCLAIMER NOTICE

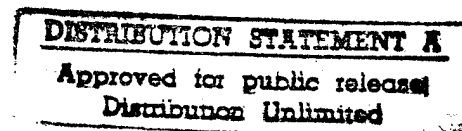


THIS DOCUMENT IS BEST QUALITY AVAILABLE. THE COPY FURNISHED TO DTIC CONTAINED A SIGNIFICANT NUMBER OF PAGES WHICH DO NOT REPRODUCE LEGIBLY.

NASA Technical Memorandum 4185

# Fracture Toughness and Crack Growth of Zerodur

Michael J. Viens  
*Goddard Space Flight Center  
Greenbelt, Maryland*



DTIC QUALITY INSPECTED 2



National Aeronautics and  
Space Administration  
Office of Management  
Scientific and Technical  
Information Division

1990

## TABLE OF CONTENTS

ABSTRACT . . . . .	1
INTRODUCTION . . . . .	1
THEORETICAL BACKGROUND . . . . .	2
TEST MATERIAL . . . . .	6
TEST SPECIMENS AND PROCEDURE . . . . .	6
RESULTS . . . . .	8
DISCUSSION . . . . .	13
CONCLUSIONS . . . . .	16
REFERENCES . . . . .	17
ADDENDUM . . . . .	19

# FRACTURE TOUGHNESS AND CRACK GROWTH PROPERTIES OF ZERODUR

## ABSTRACT

The fracture toughness and crack growth parameters of Zerodur<sup>1</sup>, a low expansion glass ceramic material, were determined. The fracture toughness was determined using indentation techniques and was found to be  $0.9 \text{ MPa}\cdot\text{m}^{1/2}$ . The crack growth parameters were determined using indented biaxial specimens subjected to static and dynamic loading in an aqueous environment. The crack growth parameters  $n$  and  $\ln(B)$  were found to be 30.7 and -6.837, respectively. The crack growth parameters were also determined using indented biaxial specimens subjected to dynamic loading in an ambient 50% relative humidity environment. The crack growth parameters  $n$  and  $\ln(B)$  at 50% relative humidity were found to be 59.3 and -17.51, respectively.

## INTRODUCTION

Zerodur<sup>1</sup> is an engineered lithium aluminosilicate glass-ceramic material which is ideal for use as telescope mirrors due to its homogeneity and low coefficient of thermal expansion [1]. The use of Zerodur is anticipated in the Advanced X-ray Astrophysics Facility (AXAF) and the Far Ultraviolet Spectroscopic Explorer (FUSE). Zerodur is also, at present, the pre-phase B baseline mirror material for the Orbiting Solar Laboratory (OSL). In order to conform to fracture control guidelines [2] the components made from the Zerodur material must be either proof tested and/or analytically shown to be capable of withstanding the anticipated loading. The work reported here was initiated to supply the necessary material dependent crack growth data to enable analytical predictions of component lifetimes to satisfy the safe-life design criteria.

To demonstrate safe-life, the initial flaw size, the flaw growth rate and the critical flaw size must be known. The initial flaw size is dependent on the manufacturing processes used to produce the component. The strength controlling flaw could be either a surface flaw created during machining the component or volume flaws created during manufacturing of the bulk material.

The strength controlling flaws in glass and ceramic components are generally one to two orders of magnitude smaller in size than those that can be located with conventional non-destructive inspection techniques. Because the inherent flaw sizes cannot be measured directly, the initial condition of the component cannot be directly determined (except for very large flaws). The flaw population must be determined indirectly using test coupons prepared with the same surface finish(es) as the flight component. A large population of coupons must be tested to accurately determine the spectrum of flaw sizes created by a given finishing technique. The flaw size then used as the initial flaw size of the component is statistically made based on test results and some acceptable level of probability. The initial flaw size must be determined on a case by case basis and no inference as to initial flaw size should be drawn from this report.

The crack growth observed in glass and ceramic materials is known to be assisted by the presence of ambient moisture. To calculate the amount of growth a flaw will undergo, the rate at which the flaw will grow in the service environment and the applied stress levels must be known.

<sup>1</sup> Shott Optical Glass Inc., Duryea, PA

The fracture toughness of the material must also be known to demonstrate safe-life. The fracture toughness of the material will dictate how much stress a component can withstand for a given flaw size, or will predict the flaw size that will induce failure for a given stress.

The primary purpose of the testing performed for this report was to determine the crack growth rate in Zerodur. The fracture toughness has also been determined using indentation techniques. While specimens were tested in the as-received condition to quantify the initial flaw size distribution, no attempt should be made to use the strength of the as-received specimens as a design parameter.

## THEORETICAL BACKGROUND

### Biaxial Loading

The use of biaxial loading to interrogate glass and ceramic materials has been well documented in recent years [3-5]. The primary advantage of this technique is the specimen cost. A cylinder with the desired diameter can be core drilled from bulk material and the disk specimens sliced off the cylinder. The specimens can then be polished to the desired surface finish. Very little attention needs to be paid to the specimen edges because the creation of the maximum stress at the center of the specimen prevents any failures from edge flaws, as is observed in three or four point bend specimens.

The stress on the tensile surface of the test specimens ( $\sigma$ ) is given as [3]:

$$\sigma = 3P[2(1+\nu)\ln(a/b)+(1-\nu)(a^2-b^2)/R^2)]/4(\pi)t^2 \quad (1)$$

where P is the applied load in newtons,  $\nu$  is the Poisson's ratio, t is the specimen thickness, a is the support ring radius, b is the loading ring radius and R is the specimen radius. The specimen dimensions are in millimeters.

The strength data at each test condition were fitted to a two parameter Weibull relationship [6]:

$$\ln \ln [1/(1-F)] = m \ln[\sigma_f/\sigma_0] \quad (2)$$

where the value  $\sigma_f$  is used to denote the specimen strength at failure, m and  $\sigma_0$  are the Weibull modulus and Weibull scale parameter, respectively. The Weibull parameters are determined by a least squares linear regression of Eq. (2) where F is the cumulative failure probability defined as,  $F=(i+0.5)/J$  (i is the specimen rank and J is the total number of specimens tested). The Weibull median strength is the fracture strength corresponding to a failure probability of 0.5 and the Weibull modulus represents the scatter in the specimen strengths.

The strength of large components can be predicted based on small specimen strengths by accounting for the difference in size or area stressed. The relationship is given as:

$$\sigma_1/\sigma_2 = (A_2/A_1)^{1/m} \quad (3)$$

where  $A$  is the area being interrogated and  $m$  is the Weibull modulus, the subscripts 1 and 2 represent the large component and test specimens, respectively. Equation (3) accounts only for surface flaws. If volume flaws are the strength controlling defects then the volume and the stress distribution in that volume must be taken into account.

### Indentation Theory

The use of indenters (Knoop and Vickers) to create well defined flaw systems (Figure 1) in glass and ceramic components has been well documented [7-14]. The variation in strength of specimens with indentation flaws is much lower than that of specimens with as-machined surfaces and is thus ideally suited for the introduction of flaws for crack growth testing. The flaws created using the indentation technique are on the scale of the as machined flaws.

The response of brittle materials when indented with a Vickers indenter is the creation of a well defined crack system driven by contact residual stress. The contact residual stress is created by a strain mismatch between the plastically deformed material adjacent to the indentation site and the elastically deformed surrounding matrix. During the indentation event two crack systems are formed; radial and lateral. The radial cracks grow perpendicular to the surface and are the flaws from which fracture occurs. The lateral flaws form at the base of the plastic zone and grow parallel to the surface.

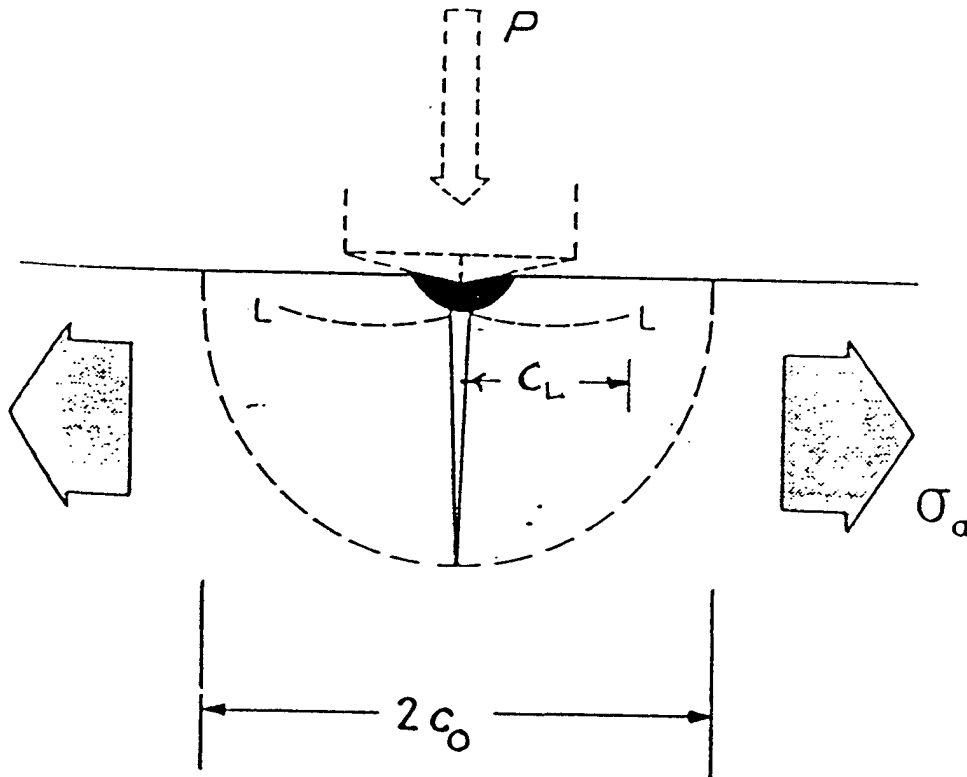


**Figure 1. Idealized model of damage created by indentation with Vickers indenter. The radial crack length is  $c_0$  and the lateral crack length is  $c_L$ . The darkened area beneath the indentation represents the plastic zone and  $\sigma_a$  is the far field applied stress (after reference [9]).**

## Fracture Toughness

### Direct Crack Method

The stress intensity at the tip of the radial crack created during indentation is determined by modelling the indentation stress field and the radial crack system as a center loaded crack. It can be shown that the radial crack dimension after indentation ( $c_0$ ) is [10]:

$$c_0 = [\chi_r P / K_{IC}]^{2/3} \quad (4)$$

where  $P$  is the indenter load,  $K_{IC}$  is the critical stress intensity factor (fracture toughness) and  $\chi_r$  is the residual stress constant that is dependent on indenter geometry and material properties. The  $\chi_r$  factor has been calibrated using a wide range of ceramic materials and was found to be equal to  $0.016 (E/H)^{1/2}$  where  $E$  is the elastic modulus and  $H$  is the hardness. Rearranging equation (4) yields the critical stress intensity as [10]:

$$K_{IC} = 0.016 [E/H]^{1/2} [P/c_0^{3/2}] \quad (5)$$

Note that the  $[P/c_0^{3/2}]$  term is a material constant. This value should be constant in the absence of a far field residual stress in the material being tested.

### Strength Method

The stress intensity at the tip of a radial crack may be found by summing the stress intensity due to residual and applied stresses. The post indentation strength is calculated at the point where crack instability occurs:  $K_I = K_{IC}$  and  $dK_I/dc > 0$ . At this point the critical stress intensity is found to be [11]:

$$K_{IC} = \eta [E/H]^{1/8} [\sigma_f P^{1/3}]^{3/4} \quad (6)$$

where  $\eta$  is a calibration constant that also incorporates the flaw geometry, assumed to be an ideal half penny shape. The  $\eta$  constant has been calibrated to be  $0.59 (\pm 0.12)$  [11].

## Crack Growth Parameters

### Static Fatigue

Crack growth of glass and ceramic materials occurs when statically loaded in an aggressive environment. The crack growth can be expressed as a power function of the stress intensity factor ( $K_I$ ) and is given as [14-17]:

$$v = v_0 (K_I / K_{IC})^n \quad (7)$$

where  $v$  is the crack velocity, and  $v_0$  &  $n$  are material and environmental crack growth constants. From the power law relationship an expression for the time to failure ( $t_f$ ) can be derived in terms of the applied stress ( $\sigma_a$ ), and is given as:

$$t_f = B \sigma_i^{n-2} \sigma_a^{-n} \quad (8)$$

$$B = 2/[v_0 Y^2 (n-2) K_{IC}(-2)] \quad (8a)$$

where  $\sigma_i$  is the strength in the absence of subcritical crack growth or inert strength and  $Y$  is a flaw geometry factor taken to be  $\pi$  for surface flaws.

The crack growth parameters  $n$  and  $B$  are found using the median time to failure and corresponding applied stress. The use of median values are convenient as they represent the time to failure at a 50% failure probability. A least squares linear regression analysis is performed on the natural logs of the median time to failure and the corresponding applied stress. The slope is the  $n$  parameter and the intercept is  $[B \sigma_i^{n-2}]$ .

### Dynamic Fatigue

Dynamic fatigue of glass and ceramic materials refers to the decrease in the observed strength as a function of decreasing stressing rate. The relationship between failure stress ( $\sigma_f$ ) and stressing rate ( $\sigma$ ) is given as:

$$\sigma_f^{n+1} = B (n+1) \sigma_i^{n-2} \sigma \quad (9)$$

The crack growth parameters  $B$  and  $n$  are determined as described above for static fatigue, using the median failure stress and the associated stressing rate.

### Fatigue of Indentation Flaws

It has been shown that the fatigue parameters determined using indentation flaws differ from those determined when the residual stress field associated with the indentation event is removed by annealing. The relationship between the apparent fatigue exponent ( $n'$ ) and actual fatigue exponent ( $n$ ) is given as [17]:

$$n = 1.31 n' \quad (10)$$

The primed notation designates the value determined in the presence of the residual stress. The relationship between the  $B$  and  $B'$  values is not as straight forward as that of  $n$ . The true value of the fatigue parameter  $v_0$  as a function of indentation load is given as [17]:

$$v_0 = [2.84 n'^{0.462} \sigma_m^{n'} c_m]/\lambda' \quad (11)$$

$$\lambda' = B' (n' + 1) \sigma_m^{(n' - 2)} \quad (11a)$$

where  $\sigma_m$  is the inert strength for a given indentation load and  $c_m$  is the corresponding radial crack size at failure and taken to be 2.5 times larger than  $c_0$ . The value for  $\sigma_m$  is taken as the inert strength in equations (8) and (9). The true  $B$  parameter can be determined by substituting values obtained in equations (10) and (11) into equation (8a).

## TEST MATERIAL

Zerodur is an opaque, engineered glass-ceramic material based on a lithium-aluminosilicate formulation with the crystalline phase consisting of metastable solid solutions of high quartz structure. Zerodur is 70 to 78% by weight crystalline phase with crystals generally 50 to 55 nanometers in size. The material composition is given in Table 1.

Table 1. Zerodur Composition\*

	<u>Composition</u>	
	wt%	mol%
SiO <sub>2</sub>	55.4	63.9
Al <sub>2</sub> O <sub>3</sub>	25.4	17.2
Li <sub>2</sub> O	3.7	8.5
Na <sub>2</sub> O	0.2	0.2
K <sub>2</sub> O	0.6	0.5
MgO	1.0	1.7
ZnO	1.6	1.3
P <sub>2</sub> O <sub>5</sub>	7.2	3.5
TiO <sub>2</sub>	2.3	2.0
ZrO <sub>2</sub>	1.8	1.0
AsO <sub>3</sub>	0.6	0.2

\* Ref. [19]

Table 2. Zerodur Mechanical Properties\*

Modulus of Elasticity (E,GPa)	91.0
Poisson's Ratio ( $\nu$ )	0.24
Density ( $\rho$ ,g/cm <sup>3</sup> )	2.53
Hardness, Knoop (H, GPa)	6.18
Strength (MPa)	90.0**

\* Manufacturers data.

\*\* 0.5 cm<sup>2</sup> test area, loaded at 2 MPa/sec, No. 600 loose grain finish, 5% failure probability.

The manufacture of the Zerodur material requires tight control of a nucleation and crystallization process which creates the material's microstructure. Annealing of sodalime glass specimens with indentation flaws has been shown to remove the localized residual stress created during the indentation event [15]. Annealing of the Zerodur specimens to remove the indentation residual stress field might have altered this microstructure, so was not performed.

Zerodur has very good thermal stability. Various thermal expansion classes are available with the most stable being expansion class 1 which has a thermal expansion coefficient of  $0 \pm 0.05$ ppm/K for 0 to 50°C.

Zerodur has good resistance to chemical attack. Zerodur resists attack by most acids (with exception of hydrofluoric acid), alkalis and salts at room temperature. Sulfuric acid does attack Zerodur at higher temperatures.

## TEST SPECIMENS AND PROCEDURE

Zerodur disks (38.1 mm dia x 1.78 mm) were used in this study. The faces were polished to a commercial grade finish by the manufacturer<sup>1</sup>. All specimens were randomized prior to testing to avoid any systematic error due to manufacturing processes.

<sup>1</sup> Shott Optical Glass Inc., Duryea, PA

## Indentation

A Vickers diamond indenter was used to introduce indentations into the Zerodur specimens at loads ranging from 300 to 2000 grams. The hardness tester<sup>2</sup> used to introduce indentations into the specimens had a constant loading rate of 6 mm/min and remained in contact for 20 seconds. Crack lengths were measured one hour after the indentation event on a Nikon Epiphot microscope at 1000 times magnification.

The indents were placed in the center of the tensile side of the specimens. The center of the specimen was located by placing the specimen on a template and placing a small fiducial "dot" in the center of the compressive face. The dot was a dry transfer lettering bullet. The center of the specimen was then located directly under the indenter. This fiducial dot also insured that the center of the specimen, and indentation, were located at the center of the loading ring. The test specimens were allowed to sit in ambient conditions for one hour prior to strength testing.

## Dynamic Testing

A biaxial test fixture mounted on a servo hydraulic test machine<sup>3</sup> was used for all dynamic strength testing. All specimens were tested with a ring on ring loading configuration (Figure 2). The loading and support rings were 5.8 and 25.4 mm diameter thrust bearings, respectively.

The use of the thrust bearings to support the specimens was preferred over machined rings for several reasons. The use of thrust bearings was felt to lessen the amount of friction on the specimen surface, there is a high degree of dimensional consistency between bearings and the cost of the thrust bearings was much less than the cost of machining several rings. The test fixtures used were easily retrofitted using the thrust bearing races. The smaller thrust bearings were used as loading rings to avoid any effect that might arise at the periphery of a ground ball and to provide dimensional consistency between loading fixtures.

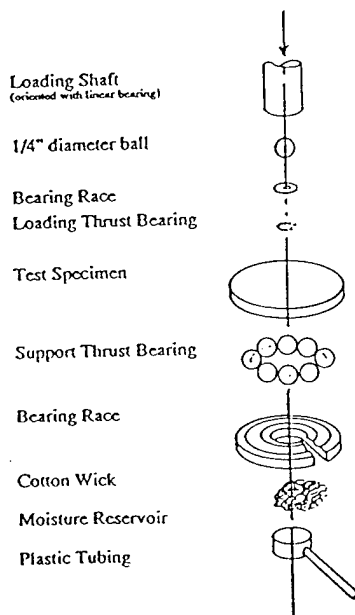


Figure 2. Schematic of test configuration.

<sup>2</sup> Tukon Tester Model FB, Wilson Instruments, Binghamton, NY

<sup>3</sup> Instron 1350, Instron Corp., Canton, MA

The inert strength of the Zerodur specimens was determined for both as-received and indented specimens. The indentation loads were 300, 500, 1000 and 2000 grams. A minimum of 10 specimens was tested at each condition. The inert strength specimens were tested in air at a loading rate of 2 millimeters/second which resulted in stressing rates of approximately 2000 MPa/sec. This loading rate was felt to be sufficient to limit the environmentally assisted crack growth.

The load was recorded using a data acquisition and plotting system<sup>4</sup>. The load was monitored with a piezoelectric load cell<sup>5</sup> at loading rates greater than 0.2 mm/sec and with a standard strain gauged load cell at loading rates less than 0.2 mm/sec. The slowest loading rate used was 5 mm/hr.

The dynamic fatigue parameters were determined for a water environment using specimens with 500 and 1000 gram Vickers indentations. The water environment was created by placing a drop of deionized water over the indentation prior to testing. The dynamic fatigue parameter was also determined for 50% relative humidity (RH) using specimens with 1000 gram indentations. The 50% RH was provided by the ambient lab environment.

### Static Testing

The static fatigue testing reported here used only two fixtures. The fixtures used for static fatigue testing were identical to that used for the dynamic fatigue testing but had a weight pan attached to the loading shaft. It was confirmed that the applied stress on the tensile surface agreed with theory using a strain gauged Zerodur specimen. The agreement with theory was within 1 percent for both fixtures.

A target stress was selected and the desired weight calculated using Eq. (1) and the individual specimen thickness. The load was applied with lead blocks and lead shot. The lead shot was weighed out to the precise load required to induce the target stress. The load was applied to the specimen via a weight pan. When specimen failure occurred the weight pan tripped a microswitch and the failure time was automatically recorded by a personal computer<sup>6</sup>.

The static fatigue specimens were tested in a deionized water environment. The water was wicked to the specimen surface from a reservoir located directly beneath the tensile surface. The reservoir was replenished as required via plastic tubing.

## RESULTS

### Hardness

The indentation diagonal sizes are presented in Table 3. The hardness, calculated as twice the applied load divided by the indentation diagonal squared (the factor of two represents the Vickers indenter geometry), was found to decrease with increasing indenter load. This variation of hardness with increasing load has been previously noted with sodalime glass [21]. The mean hardness value was found to be 6.37 GPa. This value agrees with the hardness value provided by the manufacturer (6.2 GPa).

<sup>4</sup> Hewlett Packard Measurement Plotting System (HP-7090A), Hewlett-Packard Co., Rockville MD

<sup>5</sup> Kistler Instrument Corp., Amherst NY

<sup>6</sup> COMPAQ, COMPAQ Computer Corp.,

Table 3. Indentation Dimensional Measurements

Indentation Load (grams)	Indentation Diagonal ( $\mu\text{m}$ )	Hardness (GPa)	Crack Length ( $c_0, \mu\text{m}$ )	Fracture* Toughness ( $\text{MPa}\cdot\text{m}^{1/2}$ )
300	29.2(1.1)	6.89	32.1(1.8)	0.941
500	39.2(0.9)	6.39	46.3(1.6)	0.940
1000	56.3(1.1)	6.20	74.7(3.2)	0.931
2000	80.8(2.9)	6.01	129.4(9.8)	0.830

\* Calculated using equation (5)

Numbers in parenthesis are standard deviations.

### Inert Strength

The inert strength data is presented in Table 4. The as-received strength value determined in this study can be compared to previously reported Zerodur strength (90 MPa, Table 2) by first calculating the strength at a 5% failure probability using Eq. (2) and then scaling the 5% failure probability strength to the appropriate test area using Eq. (3). Taking  $\sigma_0=197.9$  MPa and  $m=3.2$  (Table 4) the as-received strength at a 5% failure probability is 78.2 MPa. Then scaling from the  $0.264\text{ cm}^2$  area used in this study is to the  $0.5\text{ cm}^2$  area previously used the strength is 64.1 MPa. The lower strength determined from this study indicates that the surface finish was slightly better on the previously tested specimens.

Table 4. Inert Strength

Indent Load (grams)	Specimens Tested	Median Strength (MPa)	Mean Strength (MPa)	KIC* ( $\text{MPa}\cdot\text{m}^{1/2}$ )	Weibull Parameters	
					$\sigma_0$ (MPa)	$m$
As-received	18	154.9	175.2(69.)		197.9	3.2
300	10	105.9	107.2(5.6)	1.101	109.9	21.5
500	10	86.6	87.7(2.5)	1.092	89.1	36.2
1000	20	72.0	71.0(5.3)	1.141	73.5	15.6
2000	10	57.8	57.9(2.7)	1.156	59.2	24.3

\* Calculated using equation (6)

The numbers in parenthesis represent 1 standard deviation

The mean and standard deviation data are plotted in Figure 3 on a  $\ln\text{-}\ln$  plot. The line through the data in Figure 3 has a slope of  $-1/3$  with the  $[\sigma_f P^{1/3}]$  term taken to be  $152.7\text{ MPa}\cdot\text{N}^{1/3}$ . Indentation theory predicts that the strength of an indented material, in the absence of any far field residual stress, will vary as the indentation load to the  $1/3$  power. The test results are in good agreement with theory.

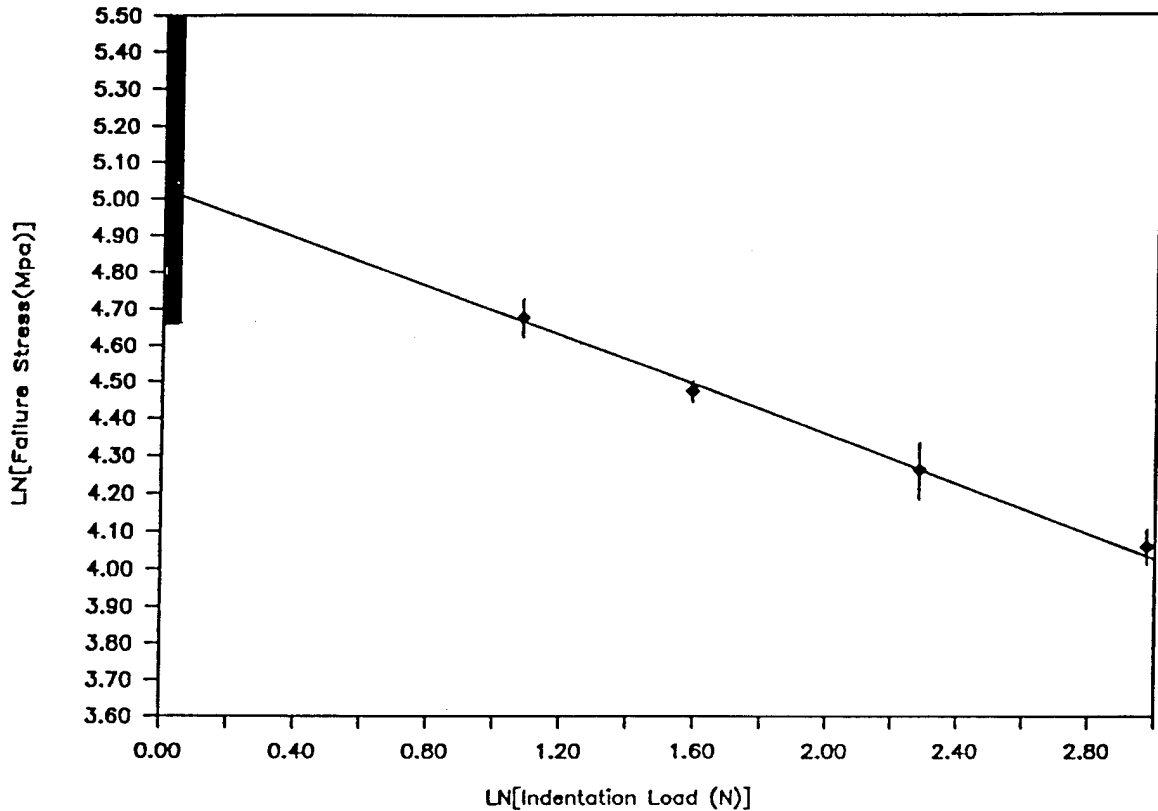


Figure 3. Inert specimen strength of the Zerodur as a function of the indentation load. The shaded area to the left represents the mean and standard deviation of the as-received specimen strength. The line through the data has a theoretical slope of  $-1/3$  with the constant  $(\sigma P^{1/3})$  value taken to be  $152.7 \text{ MPa}\cdot\text{N}^{1/3}$ .

### Fracture Toughness

The fracture toughness determined using the direct crack method and the strength method were calculated with equations (5) and (6), respectively, and are presented in Tables 3 and 4. The average fracture toughness determined by the direct crack method was  $0.911 \text{ MPa}\cdot\text{m}^{1/2}$  and the average fracture toughness determined from the strength method was  $1.123 \text{ MPa}\cdot\text{m}^{1/2}$ . These fracture toughness values are greater than previously determined using a large crack measurement technique ( $0.844 \text{ MPa}\cdot\text{m}^{1/2}$ ) [22].

### Fatigue Testing

The static fatigue median value data and associated standard deviations are plotted in Figure 4. The fatigue parameters calculated from the median value analysis of the static fatigue data are listed in Table 5. The data shown in Figure 4 at the 25 MPa applied stress was not used to calculate the fatigue parameters. Testing at this stress level is, at the time of this writing, still under way (three specimens failed prior to predicted median time to failure and two, currently being tested, have exceeded median time to failure).

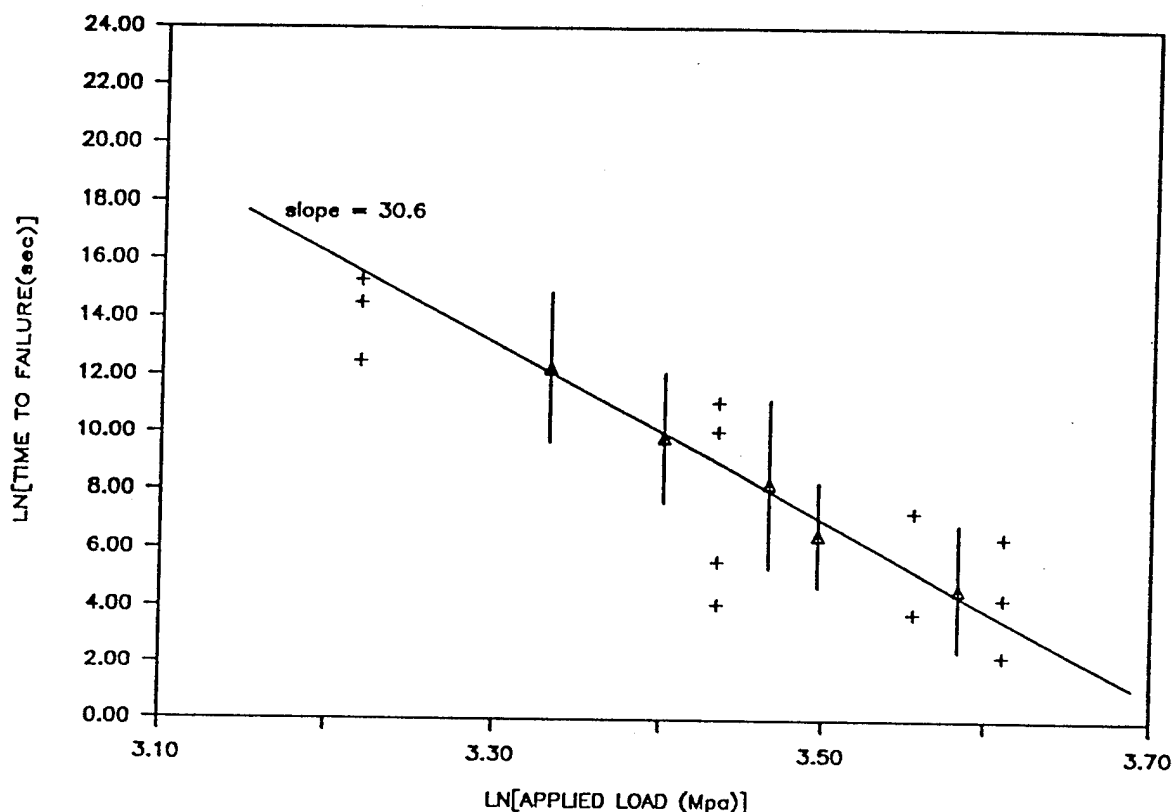


Figure 4. Static fatigue data for Zerodur with 9.8 newton indentations in a water environment. The line through the data was best fit to the median values (triangles). The error bars represent one standard deviation and the crosses represent individual failures. The specimens at 25 Mpa were not used in the regression analysis.

The results of dynamic fatigue testing using median value analysis are presented in Figures 5 and 6 and the calculated fatigue parameters are listed in Table 5. The fatigue parameter value listed for the 1000 gram indentations tested in 50% relative humidity was calculated only from specimen strengths when the rate of crack growth was dominated by the ambient moisture. These data are at the four lower stressing rates shown in Figure 6. The crack growth at the three higher stressing rates in Figure 6 is not completely controlled by ambient moisture.

Table 5. Apparent Fatigue Parameters Determined from Median Values

Indentation Load (grams)	Loading	Environment	Fatigue Parameters	
			$\ln(B')$	$n'$
500	Dynamic	Water	-2.192	23.6
1000	Dynamic	Water	-3.631	23.5
1000	Static	Water	-8.252	30.6
1000	Dynamic	50% RH	-13.885	45.2

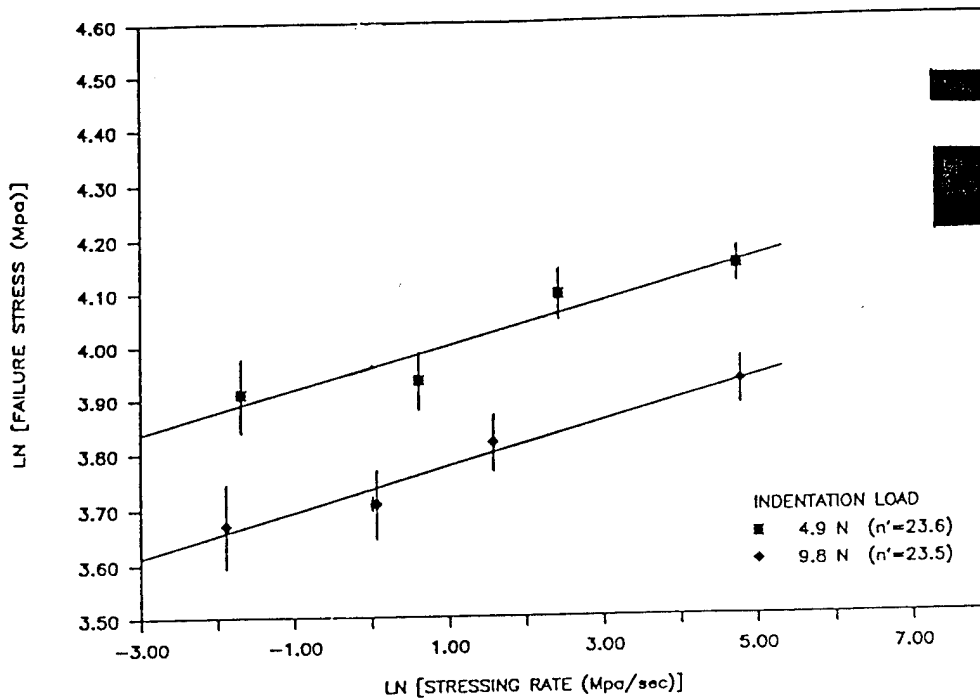


Figure 5. Dynamic fatigue data for indented Zerodur specimens in a water environment. The lines through the data are best fit to the median values for each indentation load. The shaded area to the right represent the inert strengths.

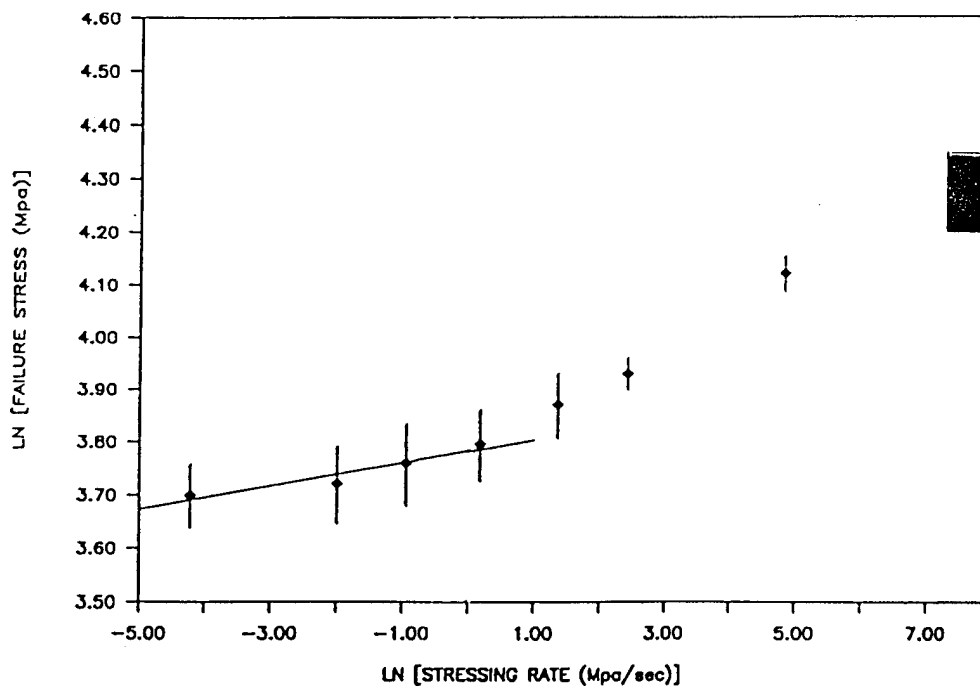


Figure 6. Dynamic fatigue data for Zerodur specimens with 9.8 newton indentations at ambient humidity (50% RH). The line through the data was best fit to the median values for at the four lower stressing rates where the crack growth is controlled by ambient moisture. The shaded area to the right represent the inert strengths.

## DISCUSSION

While the as-received strength of the specimens tested in this study should not be used as the as-received strength of flight components, it is instructive to observe the strength distribution of the specimens tested in the as-received condition. The Zerodur specimens used in this study were polished to a commercial grade finish. The Weibull plots for the inert strengths are shown in Figure 7. The distribution of the as-received strengths appears to be that of a bimodal distribution. Bimodal distributions generally occur when the strength controlling flaws come from two distinct flaw populations. These populations might be inherent voids or bubbles created during the pouring of the Zerodur and line or point flaws created by machining or handling of the specimens. The distinct flaw populations could also arise due to specimen preparation performed by different machinists, on different machines or on different days. The fracture origin could only be located in the weakest of specimens and that defect appears to be a linear flaw.

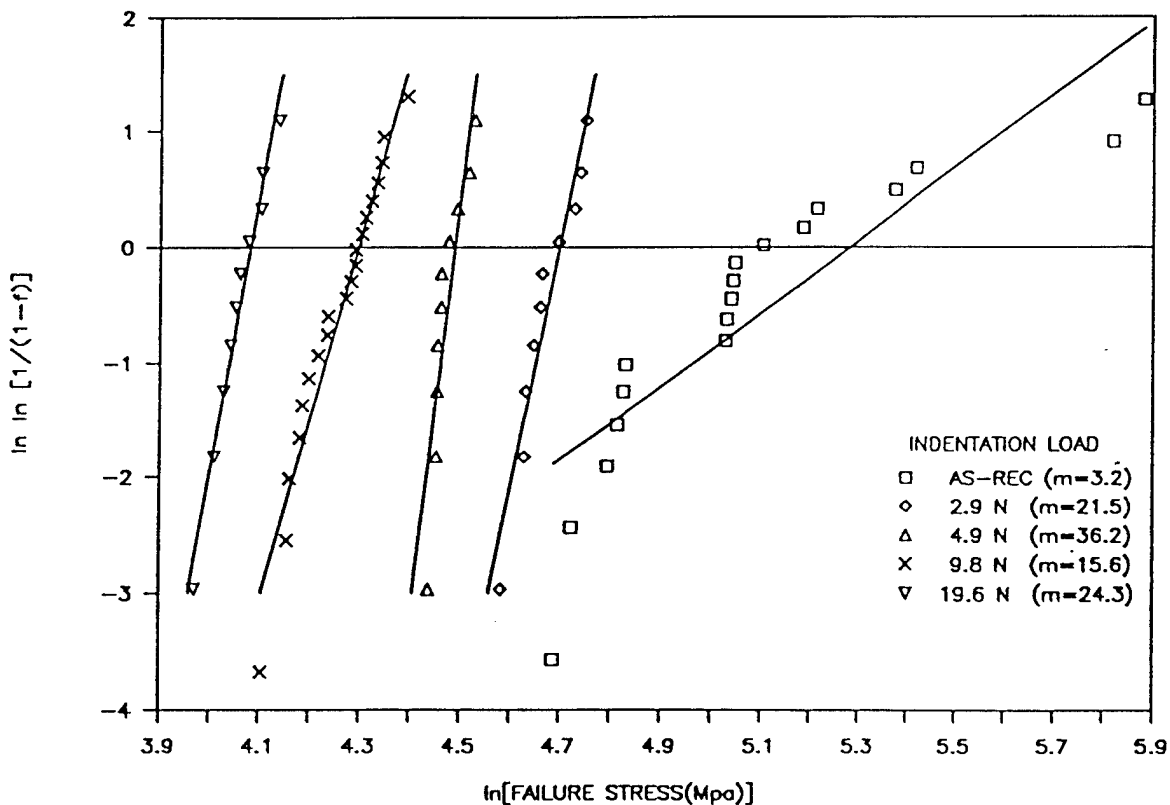


Figure 7. Weibull distribution of inert strength data.

The variation of fracture toughness values obtained from different techniques (Table 6) illustrates the uncertainty in any value obtained using a single technique. As demonstrated by the fracture toughness values determined for sodalime glass, the indentation strength technique gives an approximate fracture toughness value but is generally found to overestimate the generally accepted fracture toughness values for very low  $K_{IC}$  glass materials ( $<1\text{MPa}\cdot\text{m}^{1/2}$ ). The over estimation of the fracture toughness of glass materials by the strength method may be due to the range over which the calibration constant is obtained. The calibration constant for the strength method is determined using materials ranging from  $0.7\text{MPa}\cdot\text{m}^{1/2}$  to  $10\text{MPa}\cdot\text{m}^{1/2}$  [11]. The standard deviation associated with the calibration constant is 20% of the mean value. Due to the consistent overestimation of the fracture toughness of low  $K_{IC}$  materials when using the indentation strength technique, it would be prudent to use a twenty percent lower calibration constant to calculate the fracture toughness. Using a calibration constant of 0.47 (in place of the mean value, 0.59) in Eq.(5) the Zerodur fracture toughness determined from the strength technique is  $0.90\text{MPa}\cdot\text{m}^{1/2}$ , which is in good agreement with that determined by the direct crack method.

The fracture toughness calculated using the direct crack method was slightly greater than that using a large flaw technique. The direct crack method usually is in good agreement with the large flaw technique. The fracture toughness of sodalime glass determined by the direct crack method, using the same equipment and procedures as was used to test the Zerodur, was found to agree with values determined at other laboratories. This discrepancy may be due to the specimens originating from different material lots. To insure the component design is conservative the lower toughness value ( $0.844\text{MPa}\cdot\text{m}^{1/2}$ ) should be used for design purposes.

Table 6. Comparison of Fracture Toughness Values( $\text{MPa}\cdot\text{m}^{1/2}$ )

	Zerodur	Soda-Lime Glass	
		Ref 19	GSFC[23]
Direct Crack	0.911	0.70	0.67
Strength Method	1.123	0.94	0.94
Large Crack Method	0.844[19]	0.75	

Upon initial examination of the apparent fatigue parameters in Table 5, there appears to be poor agreement between fatigue parameters determined from static and dynamic testing. The discrepancy is eliminated when the adjusted dynamic fatigue parameters are compared to the unadjusted static fatigue parameters (Table 7). The difference observed in the fatigue parameters may be explained by the relaxation of the localized residual stress field associated with the indentation event due to the lateral crack growth during the early stages of static loading.

Recent studies have shown that the strength of sodalime glass specimens with indentation flaws increases with time after the indentation event [24]. It was observed that both the radial and lateral cracks grew during exposure to aqueous environments, but the strength increase has been attributed to the lateral crack growth relieving the localized residual stress. While the strength of the specimens tested in reference [24] did increase, the maximum strengths were less than that of the indented and annealed specimens. The strength difference between the aged and annealed specimens is attributed to the growth of the radial cracks during aging.

If it is assumed that the sustained static loading allowed the lateral cracks to grow and that the localized residual stress was relieved then the fatigue parameters determined from the static fatigue testing are the true fatigue parameters and do not need to be adjusted. The adjusted

parameters from the dynamic data agree quite well with the non adjusted parameters determined from the static fatigue testing (Table 7). The slightly lower B value for the static fatigue data may be attributed to the slightly different flaw geometry/stress field resulting from the growth of the lateral flaws; i.e. the determination of the B parameter is dependent on the inert strength value.

Table 7. Fatigue Parameters in the Absence of Residual Stress

Indentation Load (grams)	Loading	Environment	Fatigue Parameters $\ln(B)^*$	n
500	Dynamic	Water	-5.347	30.9
1000	Dynamic	Water	-6.913	30.8
1000	Static**	Water	-8.252	30.6
1000	Dynamic	50% RH	-17.51	59.2

\* True B parameter calculated using equations (8) & (11).

\*\* Static parameters not adjusted

It seems justified at this point to draw the conclusion that the results obtained using static and dynamic testing do agree. The average fatigue parameters for Zerodur in the absence of residual stresses are  $n=30.7$  and the  $\ln(B) = -6.837$ . For design purposes the B value determined from the static fatigue testing could be used to insure a conservative design. To further insure that the design is conservative the fatigue parameters determined in the presence of the indentation localized residual stress field (Table 5) could be used for life time predictions. The use of the latter parameters could allow for the presence of residual stresses created during machining of the component, which would increase the crack growth rate.

While it is necessary to insure the component will survive launch, excessive conservatism will add undesired weight to the component. The use of crack growth parameters determined in a water environment to predict component lifetimes adds a greater degree of conservatism. It is clear from the data presented in Tables 5 and 7 that the rate of crack growth in ambient moisture is much less than that in an aqueous environment. The values determined for  $\ln(B')$  and  $n'$  at 50% RH were -13.89 and 45.2, respectively. When these values are adjusted to reflect the true values,  $\ln(B)$  and  $n$  values are -17.51 and 59.2, respectively. These values are in fair agreement with values determined in reference [22] which used "...unilaterally toothed, tensile samples loaded on one axis..." in an ambient environment of 40 to 60% RH. In that reference the  $\ln(B)$  and  $n$  parameters were found to be -11.49 and 51.7, respectively. The difference in fatigue parameters may again be due to batch to batch material variations.

It is clear from the above results that the actual component environment should be taken into account during component design. Figure 8 shows curves generated using equation (8), an assumed proof stress level of 70 MPa and the parameters listed in Table 7. The initial or inert strength in equation (8) can be replaced with the proof stress and the time calculated is a minimum time to failure. The 70 MPa stress was arbitrarily selected and corresponds to a failure probability during proof stressing of 3.7%. It can be seen in Figure 8 that the variation of the B parameter does not significantly affect the lifetime analysis while the component environment does severely affect the component lifetime.

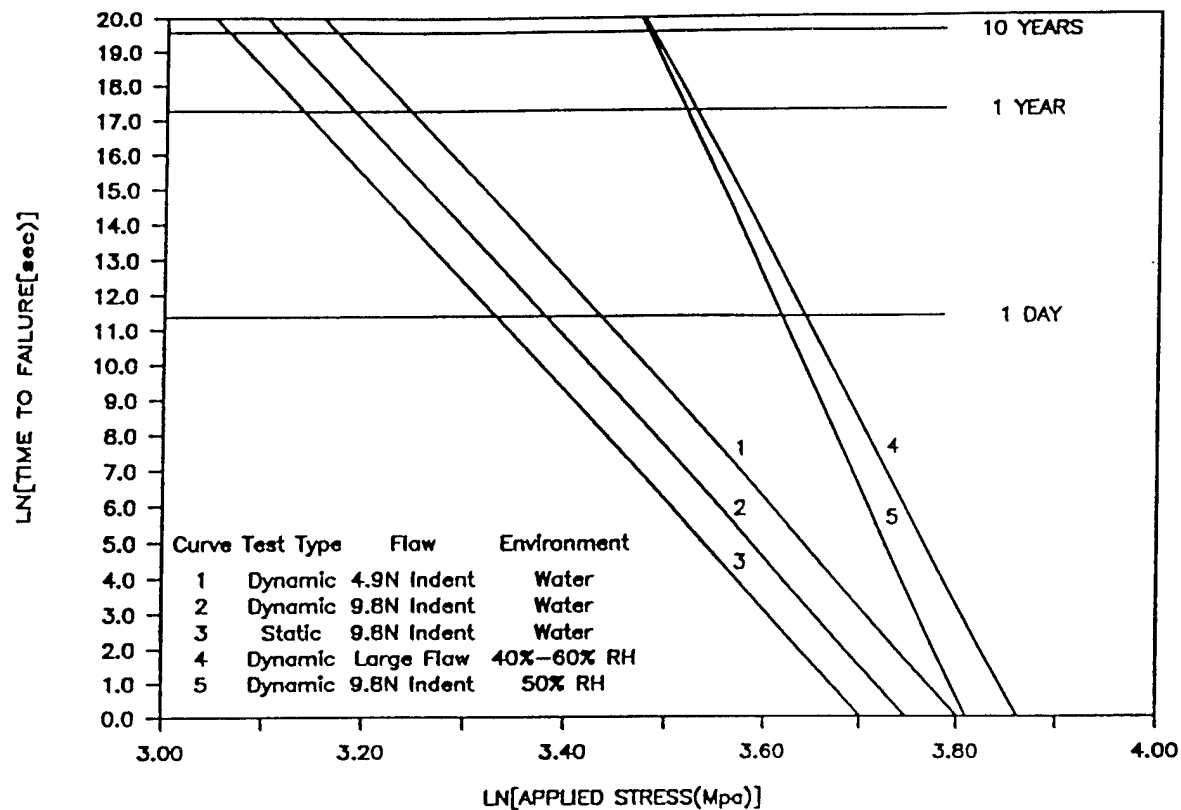


Figure 8. Median specimen lifetime calculated using fatigue parameters listed in Table 8 and in reference [22]. Inert strength was assumed to be 70 Mpa.

### CONCLUSIONS

The fracture toughness determined from this study was found to be approximately  $0.9 \text{ MPa}\cdot\text{m}^{1/2}$ . A previous study [19] using a large crack propagation technique found the fracture toughness to be  $0.844 \text{ MPa}\cdot\text{m}^{1/2}$ . It is felt the lesser value should be used to insure a conservative design.

The average true crack growth parameters  $n$  and  $\ln(B)$  for Zerodur in 100% relative humidity were determined to be 30.7 and -6.837, respectively. The true crack growth parameters  $n$  and  $\ln(B)$  for Zerodur in 50% relative humidity were determined to be 59.3 and -17.51, respectively. In the presence of a residual stress these values are considerably less.

### ACKNOWLEDGEMENTS

The author would like to thank the Far Ultraviolet Spectrographic Explorer project for supplying both the manpower and test specimens which enabled this research to be performed. The author would like to thank Mr. Heslin for his technical guidance. Implementation of the static fatigue testing was performed by Glenn Vanlandingham and Julie Brusslan.

## REFERENCES

1. H. Scheidler and E. Rodek, "Li<sub>2</sub>-Al<sub>2</sub>O<sub>3</sub>-SiO<sub>2</sub> Glass-Ceramics," Ceram. Bull., 68 [11], 1926-30 (1989).
2. Fracture Control Requirements for Payloads using the National Transport System, NBH 8071.1 September 1, 1988.
3. D.K. Shetty, et al, "Biaxial Flexure Tests for Ceramics," Ceram. Bull., 59 [12], 1193-97 (1980).
4. J.B. Watchmann, Jr, W. Capps and J. Mandel, "Biaxial Flexure Tests of Ceramic Substrates, Journal of Materials, 7 [2], 188-94 (1972).
5. J.E. Ritter, Jr, K. Jakus, A. Batakis and N. Bandyopadhyay, "Appraisal of Biaxial Strength Testing," Journal of Non-Crystalline Solids, [38-39], 419-24, (1980).
6. W. Weibull, "A Statistical Distribution Function of Wide Applicability," Journal of Applied Mechanics, [18] 293-97 (1951)
7. B.R. Lawn, A.G. Evans and D.B. Marshall, "Elastic/Plastic Indentation Damage in Ceramics: The Median/Radial Crack System," J. Am. Ceram. Soc., 63 [9-10], 554-60 (1980).
8. D.B. Marshall, B.R. Lawn and A.G. Evans, "Elastic/Plastic Indentation Damage in Ceramics: The Lateral Crack System," J. Am. Ceram. Soc., 65 [11], 561-66 (1982).
9. B.R. Lawn and T.R. Wilshaw, "Review Indentation Fracture: Principles and Applications," J. Mater. Sci., 10 [6], 1049-81 (1975).
10. G.R. Anstis, P. Chantikul, B.R. Lawn and D.B. Marshall, "A Critical Evaluation of Indentation Techniques for Measuring Fracture Toughness: I, Direct Crack Measurement," J. Am. Ceram. Soc., 64 [9], 533-38 (1981).
11. P. Chantikul, G.R. Anstis, B.R. Lawn and D.B. Marshall, "A Critical Evaluation of Indentation Techniques for Measuring Fracture Toughness: II, Strength Method," J. Am. Ceram. Soc., 64 [9], 539-43 (1981).
12. B.R. Lawn, S.w. Friedman T.L. Baker D.D. Cobb and A.C. Gonzalez, "Study of Microstructural Effects in the Strength Controlled Flaws," J. Am. Ceram. Soc., 67 [4], C67-69 (1984).
13. R.F. Cook, B.R. Lawn and C.J. Fairbanks, "Microstructure-Strength Properties on Ceramics: I, Effect of Crack Size on Toughness," J. Am. Ceram. Soc., 68 [11], 604-15 (1985).
14. D.B. Marshall and B.R. Lawn, Residual Stress Effects in Sharp Contact Cracking: Part 1, Indentation Fracture Mechanics," J. Mater. Sci., 14, 2001-12 (1979).

15. T.M. Heslin, M.B. Magida and K.A. Forrest, "A Method for Developing Design Diagrams for Ceramic and Glass Materials using Fatigue Data," NASA RP 1174, September 1986.
16. D.B. Marshall and B.R. Lawn, "Flaw Characteristics in Dynamic Fatigue: The Influence of Residual Contact Stress," J. Amer. Ceram. Soc., 63 [9-10], 532-36 (1980).
17. P. Chantikul, B.R. Lawn, and D.B. Marshall, "Micromechanics of Flaw Growth in Static Fatigue: Influence of Residual Contact Stress," J. Amer. Ceram. Soc., 64 [6], 322-25 (1981).
18. B.R. Lawn, D.B. Marshall, G.R. Anstis, and T.P. Dabbs, "Fatigue Analysis of Brittle Materials using Indentation Flaws," Journal of Materials Science, [16] 2846-54 (1981).
19. V. Maier and G. Muller, "Mechanism of Oxide Nucleation in Lithium Aluminosilicate Glass Ceramics," J. Am. Ceram. Soc., 70 [8] C176-78 (1987).
20. K. Jakus, D.C. Coyne, and J.E. Ritter, Jr, "Analysis of Fatigue Data for Life Time Predictions for Ceramic Materials," Journal of Materials Science, [13] 2071-80 (1978).
21. J.E. Ritter, Jr, F.M. Mahoney and K. Jakus, "A Comparison of Vickers and Knoop Indentations in Soda-Lime Glass," Fracture Mechanics of Ceramics, Vol. 8, Edited by R.C. Brant, A.G. Evans, D.P.H. Hasselman and F.F. Lange, Plenum Publishing Corp (1986).
22. H. Richter and G. Kleer, "Investigations on Characterizing Stability Behavior of Zerodur," Fraunhofer Institut Fuer Werkstoffmelhaik, Freiburg, Report V24/83, 1983.
23. M.J. Viens, "Implementation of Ring on Ring Flexure Testing," internal memorandum, Goddard Space Flight Center, (October, 1987)
24. B.R. Lawn, K. Jakus and A.C. Gonzales, "Sharp vs Blunt Crack Hypotheses in the Strength of Glass: A Critical Study using Indentation Flaws," J. Amer. Ceram. Soc., 68 [1], 25-34 (1985).

## ADDENDUM

### Homologous Ratio Analysis

A material's crack growth constants are generally determined using the median values, since these values are at equal failure probabilities (0.5). The median values analysis, while easy to apply, can result in large uncertainties in the B and n values. An alternate method to analyze the data is based on a homologous stress ratio ( $\sigma_{HS}$ ), given as [20]:

$$\sigma_{HS} = \sigma_a / \sigma_i \quad (11)$$

The homologous stress is ranked based on the inert strength ranking and associated with the correspondingly ranked time to failure for a given applied stress. Equation (8) is rewritten as:

$$\ln(t_f \sigma_i^2) = \ln B - n \ln \sigma_{HS} \quad (12)$$

The dynamic fatigue can be similarly analyzed by defining the homologous stress ratio to be:

$$\sigma_{HD} = \sigma_f / \sigma_i \quad (13)$$

and equation (9) can be rewritten as:

$$\ln \sigma_{HD} = (n+1)^{-1} [\ln B + \ln(n+1) + \ln(\sigma / \sigma_i^3)] \quad (14)$$

### Static Fatigue

The static fatigue data analyzed using the homologous ratio analysis technique are presented in Figure 9. The fatigue parameters determined at each applied stress and that determined using all the data are listed in Table 8. When the ranked data had unequal populations, data from the larger set were randomly selected and removed from the population, the population was then re-ranked.

The cause for the variation in the fatigue parameters obtained using the homologous ratio to analyze the static fatigue data is not certain. The homologous static fatigue parameters determined using all stress levels were close to the parameters calculated using the median values. Two individual stress levels were in excellent agreement while the other two deviated somewhat. This technique uses all the data but it is not known if there is a minimum number of data points required to insure convergence to the correct fatigue parameters.

Table 8. Fatigue Parameters Determined from Homologous Ratio Analysis of Static Fatigue Data

Applied Stress (MPa)	Fatigue Parameters $\ln(B')$	$n'$
28	-10.730	35.1
30	-8.736	30.7
32	-14.190	37.9
36	-7.645	30.9
Combined	-8.579	31.5

### Dynamic Fatigue

The homologous ratio analysis of the dynamic fatigue data at individual stress rates did not yield realistic values for the crack growth parameters. The values for the  $n$  parameter calculated from the 500 gram indentation data at individual stressing rates were negative. The  $n$  parameter calculated from the 1000 gram indentation in 100% RH varied from 4 at the 120 MPa/sec stressing rate to 21 at the 0.15 MPa/sec stressing rate. While the latter  $n$  parameter is close to that determined by the median value technique, the correlation coefficient was 0.56. The  $n$  parameter values for the 50% RH data varied from 15 to 23. These are considerably less than the value determined by the median value technique.

The regression analysis of dynamic fatigue data from all of the stressing rates, for a given indentation load and environment, using the homologous ratio gave parameters equivalent to using the median values technique. The dynamic fatigue homologous ratio data is presented in Figures 10-12.

The homologous dynamic fatigue parameters determined for individual stressing rates bore no resemblance to the values determined using the median values. The basic assumption that the homologous technique hinges on is that the strength distribution of inert specimens and specimens failing at various stressing rates describe the same flaw population: i.e. the weakest specimen at a given stressing rate will fail from the same sized initial flaw as that of the weakest inert specimen. The use of the indentation technique decreases the scatter in both inert and dynamic fatigue data. The scatter in the static fatigue time to failure is substantial even with the Vickers indentations. The poor agreement obtained using the homologous ratio analysis of the dynamic fatigue data may be attributed to the small amount of scatter in both the inert and dynamic fatigue data sets.

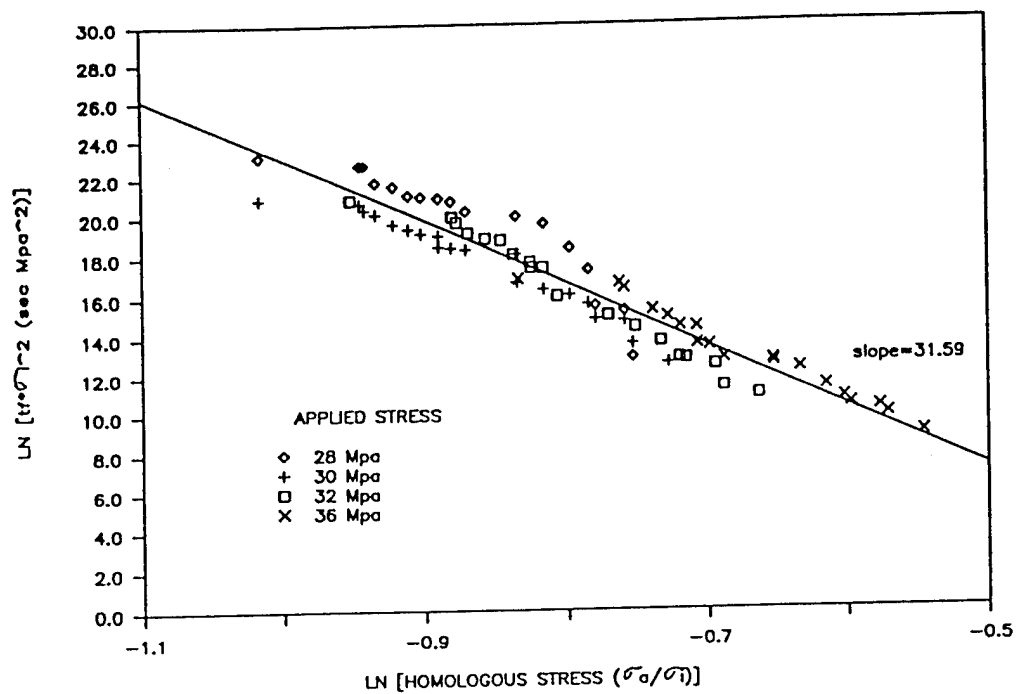


Figure 9. Static fatigue data analyzed using the homologous ratio technique. The line through the data is a best fit using all results from the four applied stresses.

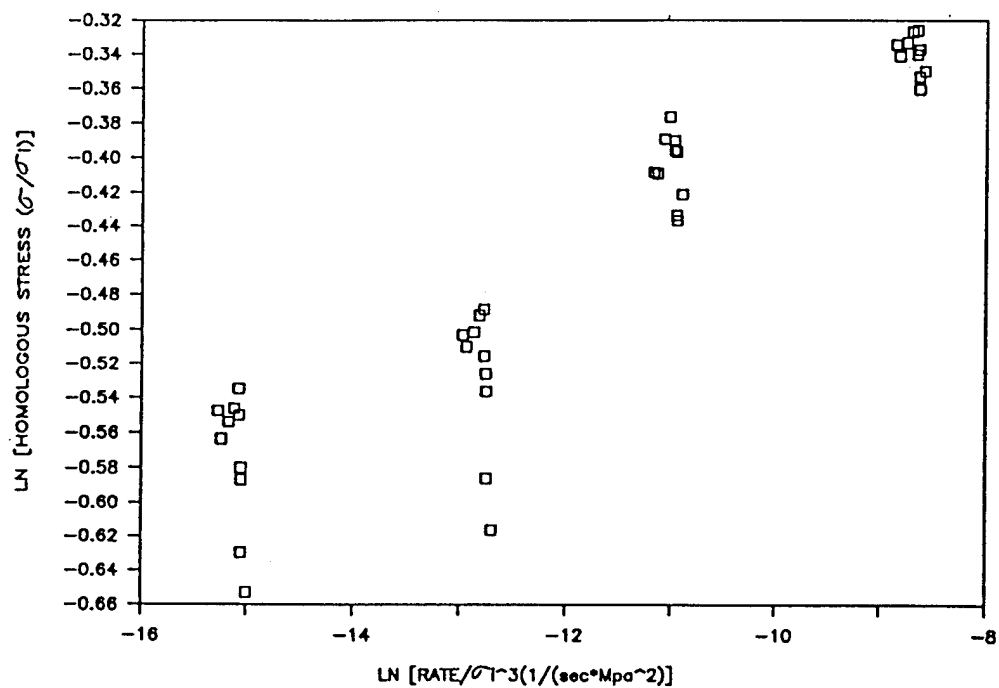
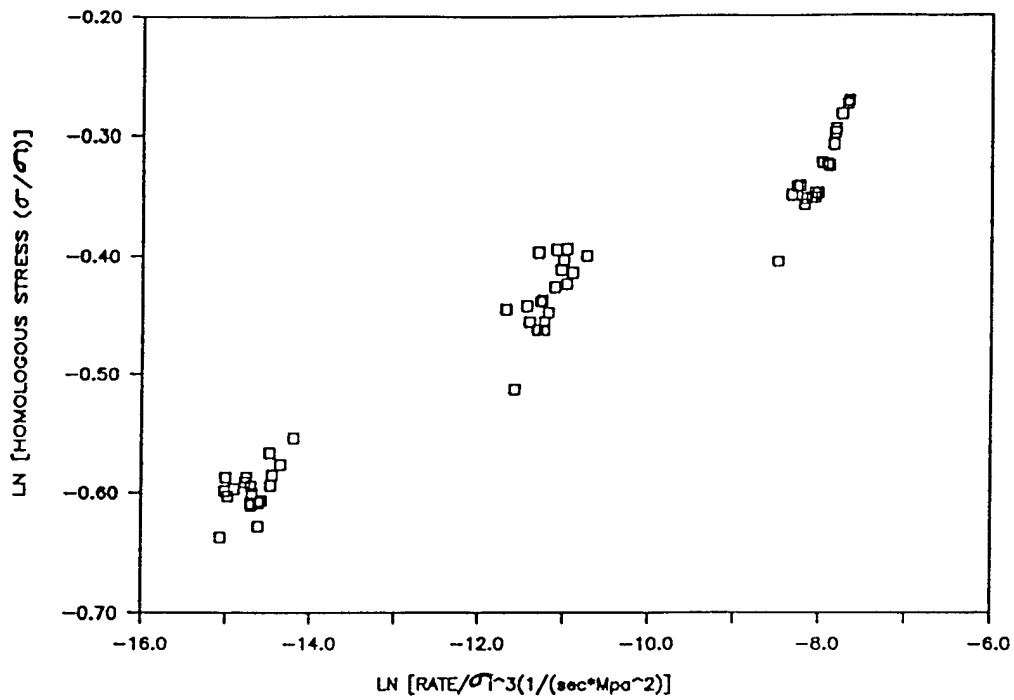
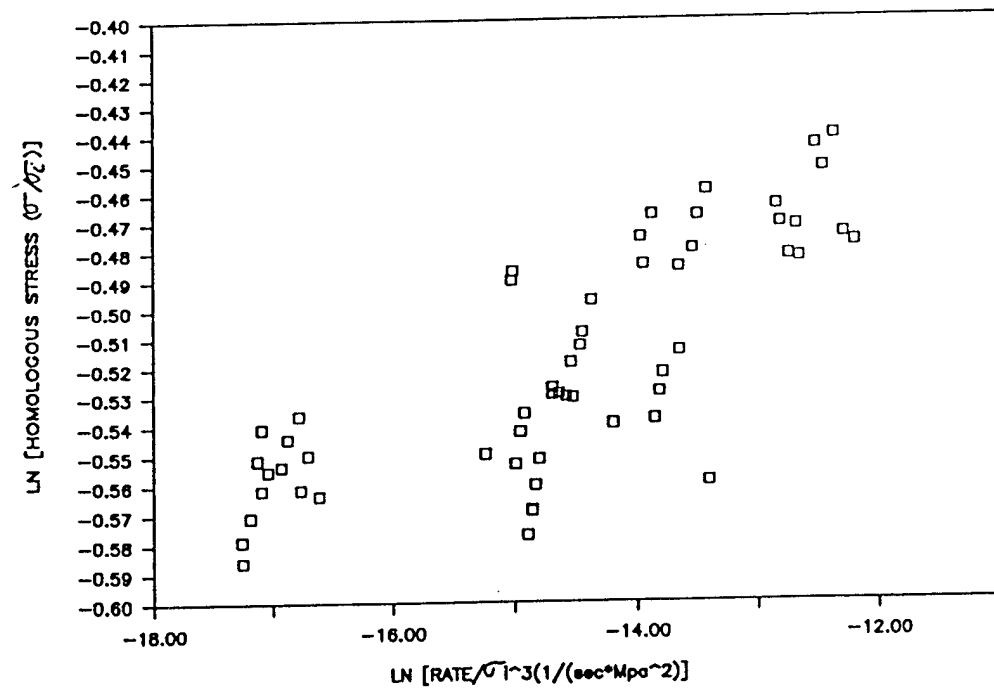


Figure 10. Dynamic fatigue data (4.9 N indentation in water) analyzed using homologous ratio technique.



**Figure 11.** Dynamic fatigue data (9.8 N indentation in water) analyzed using homologous ratio technique.



**Figure 12.** Dynamic fatigue data (9.8 N indentation in 50% RH) analyzed using homologous ratio technique.



## Report Documentation Page

1. Report No. NASA TM-4185		2. Government Accession No.		3. Recipient's Catalog No.	
4. Title and Subtitle Fracture Toughness and Crack Growth of Zerodur				5. Report Date April 1990	
				6. Performing Organization Code 90B00097	
7. Author(s)  Michael J. Viens				8. Performing Organization Report No. 313	
				10. Work Unit No.	
9. Performing Organization Name and Address National Aeronautics & Space Administration Goddard Space Flight Center Greenbelt, MD 20771				11. Contract or Grant No.	
				13. Type of Report and Period Covered Technical Memorandum	
12. Sponsoring Agency Name and Address National Aeronautics & Space Administration Washington, DC 20546-0001				14. Sponsoring Agency Code	
15. Supplementary Notes  M. Viens is affiliated with Goddard Space Flight Center, Greenbelt, MD 20771					
16. Abstract The fracture toughness and crack growth parameters of Zerodur, a low expansion glass ceramic material, were determined. The fracture toughness was determined using indentation techniques and was found to be $0.9 \text{ MPa}\cdot\text{m}^{1/2}$ . The crack growth parameters were determined using indented biaxial specimens subjected to static and dynamic loading in an aqueous environment. The crack growth parameters $n$ and $\ln(B)$ were found to be 30.7 and -6.837, respectively. The crack growth parameters were also determined using indented biaxial specimens subjected to dynamic loading in an ambient 50% relative humidity environment. The crack growth parameters $n$ and $\ln(B)$ at 50% relative humidity were found to be 59.3 and -17.51, respectively.					
17. Key Words (Suggested by Author(s))  Zerodur, lithium-aluminosilicate glass ceramic, crack growth fracture toughness			18. Distribution Statement  Unclassified - Unlimited Subject Category 27		
19. Security Classif. (of this report)  Unclassified		20. Security Classif. (of this page)  Unclassified		21. No. of pages  26	
				22. Price  A03	